Letter

# Knot topology of exceptional point and non-Hermitian no-go theorem

Haiping Hu [1,*] Shikang Sun [1,2] and Shu Chen [1,2,3]

[1] *Beijing National Laboratory for Condensed Matter Physics, Institute of Physics, Chinese Academy of Sciences, Beijing 100190, China*

[2] *School of Physical Sciences, University of Chinese Academy of Sciences, Beijing 100049, China*

[3] *Yangtze River Delta Physics Research Center, Liyang, Jiangsu 213300, China*

(Received 28 November 2021; revised 18 May 2022; accepted 30 May 2022; published 27 June 2022)

Exceptional points (EPs) are peculiar band singularities and play a vital role in a rich array of unusual optical phenomena and non-Hermitian band theory. In this Letter, we provide a topological classification of isolated EPs based on homotopy theory. In particular, the classification indicates that an $n$th order EP in two dimensions is fully characterized by the braid group $\mathrm{B}_n$, with its eigenenergies tied up into a geometric knot along a closed path enclosing the EP. The quantized discriminant invariant of the EP is the *writhe* of the knot. The knot *crossing number* gives the number of bulk Fermi arcs emanating from each EP. Furthermore, we put forward a non-Hermitian *no-go* theorem, which governs the possible configurations of EPs and their splitting rules on a two-dimensional lattice and goes beyond the previous fermion doubling theorem. We present a simple algorithm generating the non-Hermitian Hamiltonian with a prescribed knot. Our framework constitutes a systematic topological classification of the EPs and paves the way towards exploring the intriguing phenomena related to the enigmatic non-Hermitian band degeneracy.

DOI: 10.1103/PhysRevResearch.4.L022064

*Introduction.* Non-Hermitian (NH) systems are ubiquitous in physics [1–9] as epitomized by various photonic platforms with gain and loss [4,10–27]. One of the most remarkable features of NH systems is that they exhibit level degeneracy of their complex eigenenergies, called exceptional points (EPs) [28,29]. At an EP, two or more eigenvalues and their corresponding eigenvectors simultaneously coalesce (i.e., the Hamiltonian is defective), giving rise to phenomena without any analogs in the Hermitian realm. The intriguing properties of EPs have been widely exploited, such as in unconventional transmission or reflection [30], enhancing sensing [31–33], single-mode lasing [34,35], and nonreciprocal phase transitions [36].

EPs can be categorized into different types [37]. An EP is of $n$th order or $n$-fold ($\mathrm{EP}_n$) if $n$ eigenstates simultaneously coalescence, i.e., the Hamiltonian is diagonalized into an $n \times n$ Jordan normal form. Similar to the well-known Dirac point or Weyl point in Hermitian systems, the EP can be characterized by assigning an integer invariant, such as the vorticity of eigenvalues [38] or discriminant number [39]. Despite the explosive theoretical and experimental research of exceptional degeneracies during the past few years, a comprehensive understanding of their exotic features and topological classification has been achieved yet. The characterization using a discriminant number is far from satisfactory and incomplete. First, EPs of different types (especially of higher order) that cannot smoothly evolve from one to another may have the same integer invariant introduced before. Second, NH Hamiltonians generally have complex eigenenergies compared to Hermitian systems, bringing critical differences in their topological characterizations [40–44]. Near an EP, the energy levels may braid and tangle together, and a full description of EPs requires the information of their nearby braiding patterns and branch cuts, hence, they cannot be captured solely by simple integer invariants. Moreover, the richness of the band braiding near an EP may induce novel types of EPs previously unidentified.

In this Letter, we formulate a homotopic classification of EPs in arbitrary dimensional NH systems (or generic parameter space), which enables the calculation of topological invariants using the machinery well developed in algebraic topology. Particularly in two dimensions (2D), our main findings are as follows: (i) An isolated $n$th order EP is fully characterized by braid group $\mathrm{B}_n$, which reduces to integer group $\mathbb{Z}$ for $\mathrm{EP}_2$. Our classification reveals the existence of infinitely many kinds of EPs which one to one correspond to the geometry knots. (ii) We demonstrate that the quantized vorticity (or discriminant number) and the number of bulk Fermi arcs emanating from the EP is the *writhe* and *crossing number* of the knot, respectively. (iii) Based on the classification, we put forward a NH no-go theorem that goes beyond the previous fermion doubling theorem and dictates the possible configurations of EPs and their splitting rules on a 2D lattice. (iv) To facilitate experimental realizations, we show how to generate a NH Hamiltonian hosting an EP of a prescribed knot pattern. Our framework bridging the NH physics, algebraic topology, and knot theory, manifests the beauty and diversity of EPs and opens a broad avenue for investigating the exotic features of NH band degeneracies.

*hhu@iphy.ac.cn

*Homotopy classification.* Let us consider an $n$-band NH Hamiltonian $H(\boldsymbol{k}) = H(k_1, k_2, \ldots, k_d)$ of the $d$-dimensional ($d$D) system (or parameter space) and suppose an isolated $n$fold EP located at $\boldsymbol{k} = 0$. At the EP, the Hamiltonian can be brought to the Jordan normal form (for simplicity, the EP is set at zero energy unless otherwise noted). Deviating from the EP, the energy levels are separated from each other. We denote the eigenvalues and corresponding eigenvectors of $H(\boldsymbol{k})$ as $X_n = (z_1, z_2, \ldots, z_n; \psi_1, \psi_2, \ldots, \psi_n)$. As an isolated EP in $d$D can be enclosed by a $(d-1)$-dimensional [$(d-1)$D] sphere $S^{d-1}$. From the homotopy point of view, classifying the band structures near the EP is to find all the nonequivalent classes of the *nonbased* maps from $S^{d-1}$ to $X_n$, denoted as $[S^{d-1}, X_n]$. Whereas our main focus here is for isolated EPs, the classification scheme can be directly extended to some other kinds of exceptional degeneracies [45–49], such as exceptional lines in three dimensions (3D). For generic exceptional band degeneracy of dimension $d_E$ ($d_E = 0$–2 corresponds to exceptional point/line/surface, respectively), the topology can be revealed by taking a nearby surface of dimension $D_s = d - d_E - 1$ with the topological invariants carried by the homotopy invariants $[S^{D_s}, X_n]$.

The eigenvalue part is the configuration space of ordered $n$-tuples $\mathrm{Conf}_n(\mathbb{C})$. As each eigenvector is unique up to multiplying a nonzero phase factor, the eigenvector space (denoted as $\Psi$) is $\Psi \cong \mathrm{U}(n)/\mathrm{U}^n(1)$ [49]. By further removing the redundancy of permutation of eigenvalues (together with their associated eigenvectors), we have the classifying space $X_n \cong (\mathrm{Conf}_n \times \Psi)/S_n$ with $S_n$ as the symmetric group of degree $n$. Using the relations $\pi_1(\mathrm{Conf}_n) = \mathrm{PB}_n$ (pure braiding group) [50,51] and $\pi_m(\mathrm{Conf}_n) = 0$ ($m \geqslant 2$) [52], and the long sequence of homotopy relations [40,41,53], we have

$$\pi_1(X_n) = \mathrm{B}_n, \quad d = 2; \tag{1}$$

$$\pi_2(X_n) = \mathbb{Z}^{n-1}, \quad d = 3; \tag{2}$$

$$\pi_{d-1}(X_n) = \pi_{d-1}[\mathrm{U}(n)], \quad d \geqslant 4. \tag{3}$$

For $d = 2, n = 2$, the homotopy group $\mathrm{B}_2 \cong \mathbb{Z}$, consistent with the previous characterization of $\mathrm{EP}_2$ through vorticity [38] or discriminant number [39]. The above homotopy groups are all Abelian except for $d = 2, n \geqslant 3$, which is the braid group $\mathrm{B}_n$. If we travel along a circle around a 2D EP, the energy levels braid together. Equation (1) indicates that the topology of a 2D $\mathrm{EP}_n$ is entirely captured by such a braiding pattern. The ordinary nondefective point degeneracy has trivial band braidings. Equation (2) means a 3D $\mathrm{EP}_n$ is characterized by assigning a Chern number to each of the separable $n$ bands with the constraints that they sum to zero.

The nonbased map relates to the homotopy group through the action of the fundamental group [53],

$$[S^{d-1}, X_n] \cong \pi_{d-1}(X_n)/\pi_1(X_n). \tag{4}$$

The right-hand side is the orbit set. $[S^{d-1}, X_n]$ is not necessarily a group and usually decomposed into several distinct sectors, induced by the fundamental group. Whereas the nonbased homotopy can be worked out in a case-by-case manner in 2D, $[S^1, X_n]$ is the conjugacy class of the braid group $\mathrm{B}_n$ [40–42]. In fact, choosing a different starting point on the encircling path may end up with another braid, which, however, conjugate to the original one, hence, they are in the same conjugacy class. In 3D, $[S^2, X_n]$ is a collection of $n$ integer Chern numbers. Due to the unsortability of the complex energy levels, the two integer sets $[s_1, s_2, \ldots, s_n]$ and $[s_{b_1}, s_{b_2}, \ldots, s_{b_n}]$ [the set induced by the band permutation of any $b \in \pi_1(X_n)$] are identified as the same [40,41].

*Knot around EP.* In the following, we focus on 2D EPs. It turns out there is a one-to-one correspondence between the conjugacy class of braid group $\mathrm{B}_n$ and geometric knot in the solid torus [54], culminating in a *knot* classification of the EPs. Different types of EPs are represented by topologically distinct knots, thus, characterized by knot invariants [42,51], e.g., Jones polynomials [55]. Intuitively, let us take a closed path $\Gamma(\theta)$ ($\theta \in [0, 2\pi]$) surrounding the EP. Along $\Gamma$, the $\theta$-dependent energy levels $(z_1, z_2, \ldots, z_n)$ trace $n$ strands which tangle together in the 3D space spanned by (ReE, ImE, $\theta$) as depicted in Fig. 1(a). The trajectory returns to itself to form a closed knot during the $\theta$ evolution from 0 to $2\pi$ ($\theta = 0$ and $\theta = 2\pi$ is identical). The knot topology of a given EP is best represented using the braid word. It can be determined by projecting the above energy-level strings onto the $\mathrm{Im}\,E = 0$ plane. As $\theta$ evolves, the strings undergo a sequence of crossings. In Artin's notation, we label a crossing as $\tau_i$ ($\tau_i^{-1}$) if the $i$th string crosses over (under) the $(i+1)$th string from the left. $\tau_i$'s satisfy the braid relation: $\tau_i\tau_j = \tau_j\tau_i$ for $|j - i| \geqslant 2$, and $\tau_i\tau_{i+1}\tau_i = \tau_{i+1}\tau_i\tau_{i+1}$. The entire level set is specified by a product of braid operators. For example, $\tau_1^n$ corresponds to twisting two-level strands $n$ times; $n = 1$–3 represents unknot, Hopf link, and Trefoil knot, respectively. We note the difference from the one-dimensional (1D) knotted separable bands [42], here, the knots of EPs are attributed to the nontrivial nearby braiding around the band singularities.

The knot near an EP can be regarded as the roots (or nodal set) of the ChP. Denote $z = k_1 + ik_2$ and $H(z) = H(k_1, k_2)$, the ChP reads

$$f(\lambda, z) = \det[\lambda - H(z)] = \prod_{j=1}^{n}(\lambda - z_j). \tag{5}$$

The well-known complex polynomial for the $(p, q)$-torus knot is $f(\lambda, z) = \lambda^p - z^q$ with $p$ roots $z_j = z^{q/p}e^{i2\pi(j-1)/p}$, ($j = 1, 2, \ldots, p$). By tracing a closed path around the EP, the energy levels wind $q$ times around a circle in the interior of the torus and $p$ times around its axis of rotational symmetry. The simplest Hamiltonian realizing the $(p, q)$-torus knot can, thus, be chosen as

$$H_{T_{p,q}} = \begin{pmatrix} 0 & 0 & 0 & (k_1 + ik_2)^q \\ 1 & 0 & 0 & 0 \\ 0 & \ddots & \ddots & 0 \\ 0 & 0 & 1 & 0 \end{pmatrix}_{p \times p}. \tag{6}$$

Figures 1(b) and 1(c) plot the band structures of $\mathrm{EP}_2$ associated with $T_{2,1}$ (unknot) and $T_{2,3}$ (trefoil knot), respectively. The unknot case is the most studied $\mathrm{EP}_2$ in the literature.

To find the Hamiltonian for an $\mathrm{EP}_n$ with a prescribed knot (denoted as $\mathcal{K}$), we need to construct the proper ChP $f(\lambda, z)$. As $\lambda, z \in \mathbb{C}$, $f(\lambda, z)$ defines a mapping from $\mathbb{C}^2$ to $\mathbb{C}$. The energy-levels $(z_1, z_2, \ldots, z_n)$ are the nodal sets of the ChP, and the $\mathrm{EP}_n$ is the isolated singularity located at $(\lambda, z) = (0, 0)$.

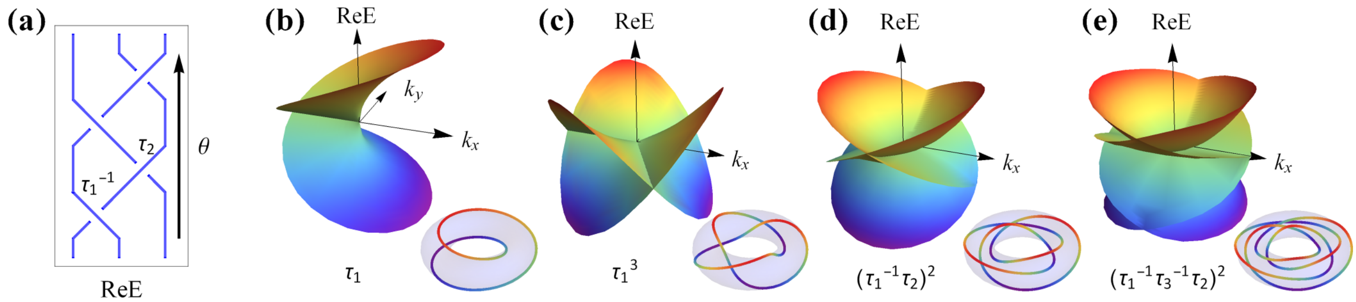


FIG. 1. Exceptional points (EPs) with energy-level braiding and knot topology. (a) Braid diagram marked by Artin's braid word notation: $\tau_i$ ($\tau_i^{-1}$) represents the $i$th strand crosses over/under the $(i+1)$th strand when traveling upwards. Closure of the braid by identifying the up and bottom ends forms a knot (in this case, it is the figure-8 knot). (b)–(e) Band structures (real part) and their associated knots along a closed path enclosing the EP (lower panels) for some representative EPs. (b) $\mathrm{EP}_2$ of unknot, braid word: $\tau_1$, the characteristic polynomial (ChP) is $\lambda^2 - z$ with $z = k_x + ik_y$; (c) $\mathrm{EP}_2$ of the trefoil knot, braid word: $\tau_1^3$, the ChP is $\lambda^2 - z^3$; (d) $\mathrm{EP}_3$ of the figure-8 knot, braid word $(\tau_1^{-1}\tau_2)^2$. The ChP for the figure-8 knot is given by $f_{F8} = 1/64[64\lambda^3 - 12\lambda a^2[3(z\bar{z})^2 + 2z^2(z\bar{z}) - 2\bar{z}^2(z\bar{z})] - 14a^3(z^2+\bar{z}^2)(z\bar{z})^2 - a^3(z^4-\bar{z}^4)(z\bar{z})]$ with $a = 1/4$; (e) $\mathrm{EP}_4$ of the $L6a1$ link, braid word: $(\tau_1^{-1}\tau_3^{-1}\tau_2)^2$.

Mathematically, the closure of the band braiding near the $\mathrm{EP}_n$ is the algebraic knot around the singular point. Akbulut and King [56] showed (albeit in a nonconstructive way) that any knot can arise as the knot around such a singular point of a polynomial in the context of complex hypersurfaces. As elaborated in Ref. [49], the desired Hamiltonian with the desired knotted EP pattern can be intuitively constructed from the Fourier parametrization of the associated braid diagram. Figure 1(d) depicts an $\mathrm{EP}_3$ with its nearby energy levels forming a figure-8 knot, described by braid word $(\tau_1^{-1}\tau_2)^2$. Figure 1(e) depicts an $\mathrm{EP}_4$ associated with the $L6a1$ link of braid word $(\tau_1^{-1}\tau_3^{-1}\tau_2)^2$. By further replacing $k_{1,2}$ with $\sin k_{x,y}$ in $H_{\mathcal{K}}(z)$, we get a 2D lattice Hamiltonian hosting the desired $\mathrm{EP}_n$ with $\mathcal{K}$ knot topology.

*Bulk Fermi arc and discriminant number.* A direct physical consequence of the EP topology is the appearance of bulk Fermi arcs [57]. For example, a pair of EPs split from a Dirac point is connected by an open-ended Fermi arc as identified as the isofrequency contour in photonic experiments [57]. Here we extend this notion to generic higher-order EPs and define the bulk Fermi arcs as the loci in the $(k_1, k_2)$ space when any two levels have the same real energy, i.e., $\mathrm{Re}[z_i] = \mathrm{Re}[z_j]$ for $i \neq j$. As the EP satisfies this condition, a bulk Fermi arc must start from an EP and end at another; The EPs are the end points of Fermi arcs. The constraint imposed by the condition $\mathrm{Re}[z_i] = \mathrm{Re}[z_j]$ yields some 1D loci in the $(k_1, k_2)$ space. The bulk Fermi arcs trace open-ended curves emanating from the EPs. From the braid representation, the bulk Fermi arc is formed whenever there is a crossing either over or under in the braid diagram. Hence, we have

$$n_{\mathrm{arc}} = n_+ + n_- = c(\mathcal{K}). \tag{7}$$

Here $n_\pm$ denotes the number of over/under crossings, respectively. $c(\mathcal{K})$ is the knot crossing number. The number of Fermi arcs $n_{\mathrm{arc}}$ emanating from each EP equals to $c(\mathcal{K})$ associated with the EP.

Moreover, the braid crossing dictates the discriminant invariant $\nu$ [39]. In its neat form, $\nu$ is the sum of band vorticity [38] for any pair of band,

$$\nu = -\frac{1}{2\pi}\sum_{i\neq j}\oint_\Gamma \nabla_{\boldsymbol{k}} \arg(z_i - z_j)\cdot d\boldsymbol{k}. \tag{8}$$

Along the closed path $\Gamma$, the EP knot contributes to the vorticity through braid crossings. An over/under crossing contributes a $\pm 1$, yielding

$$\nu = n_+ - n_- = W(\mathcal{K}), \tag{9}$$

where $W(\mathcal{K}) \equiv n_+ - n_-$ is the writhe of the knot $\mathcal{K}$. It is obvious two different EPs of different braids may have the same discriminant number, e.g., figure-8 knot and Borromean ring ($L6a4$). We stress that, the full information of an EP is encoded in its knot structure; either the bulk Fermi arc or discriminant number is determined by the braiding and has limited discriminant power to specify an EP.

*No-go theorem.* The knot classification assigns a specific braiding pattern to a given EP. On a 2D lattice, there may exist multiple different EPs featuring distinct braidings. So what kind of EP configurations is allowed? It turns out the possible EPs on a 2D lattice are governed by the following *no-go theorem*:

$$b_1 b_2 \cdots b_J \in [\mathrm{B}_n, \mathrm{B}_n], \tag{10}$$

where $J$ is the total number of isolated EPs in the 2D Brillouin zone (BZ) [see Fig. 2(a)], $b_j$ is the braid for the $j$th EP along a small surrounding path. $[\mathrm{B}_n, \mathrm{B}_n] = \{uvu^{-1}v^{-1} | (u, v) \in \mathrm{B}_n\}$ is the commutator subgroup. It is easy to check taking a conjugate element of any $b_i$, or switching its order in Eq. (10) is irrelevant [58]. We can continuously expand and deform the enclosing path to the BZ boundary as sketched in Fig. 2(a) without passing through any singularity. The resulting overall band braiding $b_1 b_2 \cdots b_J$ equals to the band braiding $cdc^{-1}d^{-1}$ along the four edges of the BZ as the upper (left) and lower (right) edge are identical. Specifically, if the two neighboring braidings $c, d$ (or two braidings along any orthogonal line cut of the BZ) commute, the composite braiding must be trivial $b_1 b_2 \cdots b_J = \mathrm{I}$.

The no-go theorem indicates that the braiding of the EP inside the BZ is determined by that of the boundary. It dictates the possible braiding configurations of the isolated EPs and imposes strong constraints on their splittings: the no-go theorem holds for all the isolated split EPs, e.g., a Dirac point splits into two EPs of opposite charges. Note that the commutator subgroup is the set of braids with total exponent sum zero in the braid generator $\tau_i$. According to Eq. (9), the doubling

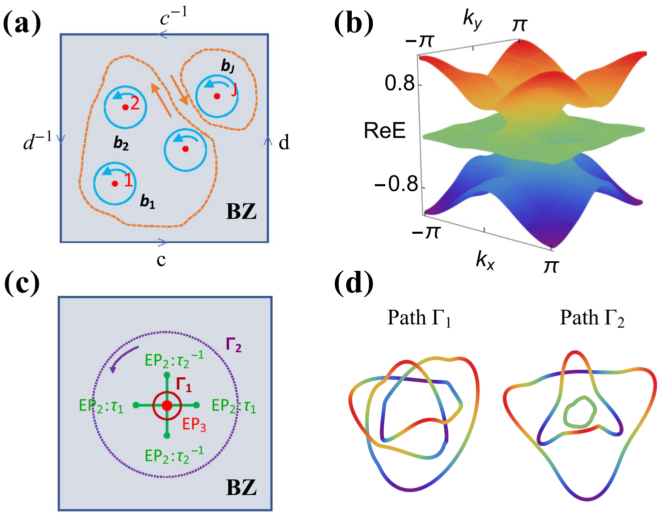


FIG. 2. Non-Hermitian no-go theorem on a 2D lattice. (a) Sketch of the proof of the theorem. The $j$th EP ($j = 1, 2, \ldots, J$) is labeled by level braiding $b_j$ along the nearby path (cyan). The paths can be continuously deformed to the orange curves and finally to the BZ boundary. (b) Band structure of model (11). $m = 0.3$. (c) EPs and their associated Fermi arcs. The $EP_3$ of the figure-8 knot (red dot) at the origin connects with the four neighboring twofold EPs (green dots) through bulk Fermi arcs (green lines). (d) Knots formed along the red path $\Gamma_1$ (left panel) and purple path $\Gamma_2$ (right panel) in (c).

theorem [39] naturally arises: The sum of the discriminant number of all EPs vanishes. Hence, a single EP of a nonzero discriminant invariant must be paired with another one of opposite discriminant number.

We illustrate the no-go theorem through an explicit model,

$$H = H_{F8} + m\begin{pmatrix} c_{x,y} & 0 \\ 1 - c_{x,y} & -c_{x,y} \end{pmatrix} \oplus 0_{1\times 1}, \qquad (11)$$

with $c_{x,y} = 2 - \cos k_x - \cos k_y$. Here $H_{F8}$ is the $3 \times 3$ lattice Hamiltonian [49] of the figure-8 EP. Without the second term, $H_{F8}$ hosts four $EP_3$ located at (0,0), $(0, \pi)$, $(\pi, 0)$, and $(\pi, \pi)$, respectively. For a finite $m$, only the $EP_3$ at (0,0) survives. A typical band structure is depicted in Figs. 2(b) and 2(c) for $m = 0.3$. Besides the $EP_3$ of the figure-8 knot with the braid word $(\tau_1^{-1}\tau_2)^2$ at the origin, four isolated twofold EPs with the braid words $\tau_1$, $\tau_2^{-1}$, $\tau_1$, and $\tau_2^{-1}$, respectively, emerge nearby. Each $EP_2$ connects to the central $EP_3$ through a bulk Fermi arc. The number of Fermi arcs emanating from each EP coincides with the knot crossing number [see Eq. (7)]. The knot along a closed path is shown in Fig. 2(d). If the loop is small, enclosing only the central $EP_3$, the energy levels close to a figure-8 knot. In contrast, if the loop encloses all the EPs, the knot is composed of three unlinked components (i.e., trivial braiding) since $\tau_2^{-1}\tau_1(\tau_1^{-1}\tau_2)^2\tau_2^{-1}\tau_1 = \mathrm{I}$, consistent with the no-go theorem.

*Discussions.* To conclude, we have established a homotopy classification of isolated EPs and demonstrated that the knots tied up by energy levels fully characterize the 2D EPs. Based on this classification scheme, we have demonstrated how to construct NH Hamiltonians corresponding to a given knot. We further proposed a no-go theorem for the EPs on a 2D lattice. Our scheme elegantly relates the bulk Fermi arc, discriminant number to the crossing number, and writhe of the knot, respectively. It is worth mentioning that the knot topology we presented refers to the knotted structures intrinsic to non-Hermitian EPs from the homotopy perspective, which should not be confused with the usual topological phase in the presence of a well-defined chemical potential. Transitions between different kinds of knotted EPs must be through band touching and rearranging.

The various EP knots and their associated NH Hamiltonians could, in principle, be realized in platforms, such as photonic lattice [25,59,60] or electric circuits [61–65]. For the former, the asymmetric coupling between the ring resonators can be implemented via auxiliary microring cavities. The consequent bulk Fermi arcs should be extracted through resonances in frequencies [57]. For the latter, the NH Hamiltonian is simulated by the circuit Laplacian, with its band structures given by the admittance spectra. We note that the model Hamiltonian in Eq. (11) no-go theorem is merely chosen for illustrative purpose of the no-go theorem and the figure-8 EP therein requires the fine-tuning of parameters. However, the stability of such knotted EPs can, in fact, be ensured by, e.g., parity time, chirality-parity, pseudo-Hermiticity, pseudochirality symmetries [66,67] due to the symmetry reduction of constraints of EPs. Under a symmetry-breaking perturbation, the knotted EP may locally split into other types of band singularities, however, the geometry knot formed by encircling the overall band singularities after splitting remains unchanged as dictated by the no-go theorem. The various knotted EPs discovered here should naturally emerge as the critical point of the nonreciprocal phase transition [36]. Beyond the isolated EPs considered here, more intricate line or surface degeneracies may exist. For example, in 2D, encircling the EP line yields the so-called singular knots. It would be interesting to extend the analysis to such singular knots and reveal their physical consequences.

*Acknowledgments.* This work was supported by the NSFC under Grants No. 11974413 and No. T2121001, the Strategic Priority Research Program of Chinese Academy of Sciences under Grant No. XDB33000000, and the start-up grant of IOP-CAS (H.H.).

[1] C. M. Bender, Making sense of non-Hermitian Hamiltonians, Rep. Prog. Phys. **70**, 947 (2007).

[2] I. Rotter, A non-Hermitian Hamilton operator and the physics of open quantum systems, J. Phys. A: Math. Theor. **42**, 153001 (2009).

[3] V. M. Martinez Alvarez, J. E. Barrios Vargas, M. Berdakin, and L. E. F. Foa Torres, Topological states of non-Hermitian systems, Eur. Phys. J.: Spec. Top. **227**, 1295 (2018).

[4] R. El-Ganainy, K. G. Makris, M. Khajavikhan, Z. H. Musslimani, S. Rotter, and D. N. Christodoulides, Non-Hermitian physics and PT symmetry, Nat. Phys. **14**, 11 (2018).

[5] E. J. Bergholtz, J. C. Budich, and F. K. Kunst, Exceptional Topology of Non-Hermitian Systems, Rev. Mod. Phys. **93**, 015005 (2021).

[6] N. Moiseyev, *Non-Hermitian Quantum Mechanics* (Cambridge University Press, New York, 2011).

[7] A. Ghatak and T. Das, New topological invariants in non-Hermitian systems, J. Phys.: Condens. Matter **31**, 263001 (2019).

[8] L. E. F. Foa Torres, Perspective on Topological States of Non-Hermitian Systems, J. Phys. Mater. **3**, 014002 (2020).

[9] Y. Ashida, Z. Gong, and M. Ueda, Non-Hermitian Physics, Adv. Phys. **69**, 249 (2020).

[10] K. G. Makris, R. El-Ganainy, D. N. Christodoulides, and Z. H. Musslimani, Beam Dynamics in $\mathcal{PT}$ Symmetric Optical Lattices, Phys. Rev. Lett. **100**, 103904 (2008).

[11] A. Regensburger, C. Bersch, M.-A. Miri, G. Onishchukov, D. N. Christodoulides, and U. Peschel, Parity-time synthetic photonic lattices, Nature (London) **488**, 167 (2012).

[12] B. Peng, . K. Özdemir, S. Rotter, H. Yilmaz, M. Liertzer, F. Monifi, C. M. Bender, F. Nori, and L. Yang, Loss-induced suppression and revival of lasing, Science **346**, 328 (2014).

[13] H. Jing, S. K. Özdemir, X.-Y. Lü, J. Zhang, L. Yang, and F. Nori, $\mathcal{PT}$-Symmetric Phonon Laser, Phys. Rev. Lett. **113**, 053604 (2014).

[14] S. Malzard, C. Poli, and H. Schomerus, Topologically Protected Defect States in Open Photonic Systems with Non-Hermitian Charge-Conjugation and Parity-Time Symmetry, Phys. Rev. Lett. **115**, 200402 (2015).

[15] J. M. Zeuner, M. C. Rechtsman, Y. Plotnik, Y. Lumer, S. Nolte, M. S. Rudner, M. Segev, and A. Szameit, Observation of a Topological Transition in the Bulk of a Non-Hermitian System, Phys. Rev. Lett. **115**, 040402 (2015).

[16] L. Xiao, K. Wang, X. Zhan, Z. Bian, K. Kawabata, M. Ueda, W. Yi, and P. Xue, Observation of Critical Phenomena in Parity-Time-Symmetric Quantum Dynamics, Phys. Rev. Lett. **123**, 230401 (2019).

[17] L. Xiao, T. Deng, K. Wang, Z. Wang, W. Yi, and P. Xue, Observation of Non-Bloch Parity-Time Symmetry and Exceptional Points, Phys. Rev. Lett. **126**, 230402 (2021).

[18] B. Zhen, C. W. Hsu, Y. Igarashi, L. Lu, I. Kaminer, A. Pick, S.-L. Chua, J. D. Joannopoulos, and M. Soljačić, Spawning rings of exceptional points out of Dirac cones, Nature (London) **525**, 354 (2015).

[19] C. Poli, M. Bellec, U. Kuhl, F. Mortessagne, and H. Schomerus, Selective enhancement of topologically induced interface states in a dielectric resonator chain, Nat. Commun. **6**, 6710 (2015).

[20] S. Weimann, M. Kremer, Y. Plotnik, Y. Lumer, S. Nolte, K. G. Makris, M. Segev, M. C. Rechtsman, and A. Szameit, Topologically protected bound states in photonic paritytime-symmetric crystals, Nature Mater. **16**, 433 (2017).

[21] P. St-Jean, V. Goblot, E. Galopin, A. Lemaître, T. Ozawa, L. Le Gratiet, I. Sagnes, J. Bloch, and A. Amo, Lasing in topological edge states of a one-dimensional lattice, Nat. Photonics **11**, 651 (2017).

[22] L. Xiao *et al.*, Observation of topological edge states in parity-time-symmetric quantum walks, Nat. Phys. **13**, 1117 (2017).

[23] X. Zhan, L. Xiao, Z. Bian, K. Wang, X. Qiu, B. C. Sanders, W. Yi, and P. Xue, Detecting Topological Invariants in Nonunitary Discrete-Time Quantum Walks, Phys. Rev. Lett. **119**, 130501 (2017).

[24] Christian E. Rüter, K. G. Makris, R. El-Ganainy, D. N. Christodoulides, M. Segev, and D. Kip, Observation of paritytime symmetry in optics, Nat. Phys. **6**, 192 (2010).

[25] H. Hu, E. Zhao, and W. V. Liu, Dynamical signatures of point-gap Weyl semimetal, arXiv:2107.02135.

[26] J. Bartlett, H. Hu, and E. Zhao, Illuminating the bulk-boundary correspondence of a non-Hermitian stub lattice with Majorana stars, Phys. Rev. B **104**, 195131 (2021).

[27] M. Michael Denner, A. Skurativska, F. Schindler, M. H. Fischer, R. Thomale, T. Bzdušek, and T. Neupert, Exceptional topological insulators, Nat. Commun. **12**, 5681 (2021).

[28] W. D. Heiss, The physics of exceptional points, J. Phys. A: Math. Theor. **45**, 444016 (2012).

[29] M.-A. Miri and A. Alu, Exceptional points in optics and photonics, Science **363**, eaar7709 (2019).

[30] Z. Lin, H. Ramezani, T. Eichelkraut, T. Kottos, H. Cao, and D. N. Christodoulides, Unidirectional Invisibility Induced by PT-Symmetric Periodic Structures, Phys. Rev. Lett. **106**, 213901 (2011).

[31] J. Wiersig, Sensors operating at exceptional points: General theory, Phys. Rev. A **93**, 033809 (2016).

[32] W. Chen, S. K. Özdemir, G. Zhao, J. Wiersig, and L. Yang, Exceptional points enhance sensing in an optical microcavity, Nature (London) **548**, 192 (2017).

[33] M. P. Hokmabadi, A. Schumer, D. N. Christodoulides, and M. Khajavikhan, Non-Hermitian ring laser gyroscopes with enhanced Sagnac sensitivity, Nature (London) **576**, 70 (2019).

[34] H. Hodaei, M.-A. Miri, M. Heinrich, D. N. Christodoulides, and M. Khajavikhan, Paritytimesymmetric microring lasers, Science **346**, 975 (2014).

[35] L. Feng, Z. J. Wong, R.-M. Ma, Y. Wang, and X. Zhang, Single-mode laser by parity-time symmetry breaking, Science **346**, 972 (2014).

[36] M. Fruchart, R. Hanai, P. B. Littlewood, and V. Vitelli, Non-reciprocal phase transitions, Nature (London) **592**, 363 (2021).

[37] K. Kawabata, T. Bessho, and M. Sato, Classification of Exceptional Points and Non-Hermitian Topological Semimetals, Phys. Rev. Lett. **123**, 066405 (2019).

[38] H. Shen, B. Zhen, and L. Fu, Topological Band Theory for Non-Hermitian Hamiltonians, Phys. Rev. Lett. **120**, 146402 (2018).

[39] Z. Yang, A. P. Schnyder, J. Hu, and C. K. Chiu, Fermion Doubling Theorems in Two-Dimensional Non-Hermitian Systems for Fermi Points and Exceptional Points, Phys. Rev. Lett. **126**, 086401 (2021).

[40] C. C. Wojcik, X.-Q. Sun, T. Bzdusek, and S. Fan, Homotopy characterization of non-Hermitian Hamiltonians, Phys. Rev. B **101**, 205417 (2020).

[41] Z. Li and R. S. K. Mong, Homotopical classification of non-Hermitian band structures, Phys. Rev. B **103**, 155129 (2021).

[42] H. Hu and E. Zhao, Knots and Non-Hermitian Bloch Bands, Phys. Rev. Lett. **126**, 010401 (2021).

[43] K. Wang, A. Dutt, C. C. Wojcik, and S. Fan, Topological complex-energy braiding of non-Hermitian bands, Nature (London) **598**, 59 (2021).

[44] S. Yao and Z. Wang, Edge States and Topological Invariants of Non-Hermitian Systems, Phys. Rev. Lett. **121**, 086803 (2018).

[45] J. Carlström, M. Stålhammar, J. C. Budich, and E. J. Bergholtz, Knotted non-Hermitian metals, Phys. Rev. B **99**, 161115(R) (2019).

[46] M. Stålhammar, L. Rødland, G. Arone, J. C. Budich, and E. J. Bergholtz, Hyperbolic Nodal Band Structures and Knot Invariants, SciPost Phys. **7**, 019 (2019).

[47] M. Stålhammar and E. J. Bergholtz, Classification of exceptional nodal topologies protected by PT symmetry, Phys. Rev. B **104**, L201104 (2021).

[48] J. C. Budich, J. Carlström, F. K. Kunst, and E. J. Bergholtz, Symmetry-protected nodal phases in non-Hermitian systems, Phys. Rev. B **99**, 041406(R) (2019).

[49] See Supplemental Material at http://link.aps.org/supplemental/10.1103/PhysRevResearch.4.L022064 for more details on; (I) the classification scheme of exceptional degeneracy from homotopy perspective; (II) the homotopy equivalence between space $U(n)/U^n(1)$ and $GL(n,\mathbb{C})/C^{*n}$; and (III) the construction of the characteristic polynomial and its associated Hamiltonian for a prescribed knotted EP.

[50] J. S. Birman and J. Cannon, *Braids, Links, and Mapping Class, Groups* (Princeton University Press, Princeton, 1974).

[51] L. H. Kauffman, *Knots and Physics*, 3rd ed. (World Scientific, Singapore, 2001).

[52] E. Fadell and L. Neuwirth, Configuration spaces, Math. Scand. **10**, 111 (1962).

[53] A. Hatcher, *Algebraic Topology* (Cambridge University Press, Cambridge, UK, 2002).

[54] C. Kassel and V. Turaev, *Braid Groups* (Springer, Berlin, 2008), see Theorem 2.1 on p. 54.

[55] V. F. R. Jones, A polynomial invariant for knots via von Neumann algebras, Bull. Amer. Math. Soc. **12**, 103 (1985).

[56] S. Akbulut and H. King, All knots are algebraic, Commentarii Mathematici Helvetici **56**, 339 (1981).

[57] H. Zhou, C. Peng, Y. Yoon, C. W. Hsu, K. A. Nelson, L. Fu, J. D. Joannopoulos, M. Soljačić, and B. Zhen, Observation of bulk Fermi arc and polarization half charge from paired exceptional points, Science **359**, 1009 (2018).

[58] This is due to the fact that for any $x, y \in \mathrm{B}_n$, (1) $x[u, v]x^{-1} = [xux^{-1}, xvx^{-1}] \in [\mathrm{B}_n, \mathrm{B}_n]$; (2) $yb_1y^{-1}b_2\cdots b_J = (yb_1y^{-1}b_1^{-1})(b_1b_2\cdots b_J) = [y, b_1][u, v] \in [\mathrm{B}_n, \mathrm{B}_n]$; and (3) $b_{i+1}b_i = b_i^{-1}(b_ib_{i+1})b_i$.

[59] S. Longhi, D. Gatti, and G. D. Valle, Robust light transport in non-Hermitian photonic lattices, Sci. Rep. **5**, 13376 (2015).

[60] S. Mittal, V. V. Orre, G. Zhu, M. A. Gorlach, A. Poddubny, and M. Hafezi, Photonic quadrupole topological phases, Nat. Photonics **13**, 692 (2019).

[61] S. Imhof *et al.*, Topolectrical-circuit realization of topological corner modes, Nat. Phys. **14**, 925 (2018).

[62] T. Helbig, T. Hofmann, C. H. Lee, R. Thomale, S. Imhof, L. W. Molenkamp, and T. Kiessling, Band structure engineering and reconstruction in electric circuit networks, Phys. Rev. B **99**, 161114(R) (2019).

[63] E. Zhao, Topological circuits of inductors and capacitors, Ann. Phys. **399**, 289 (2018).

[64] C. H. Lee, S. Imhof, C. Berger, F. Bayer, J. Brehm, L. W. Molenkamp, T. Kiessling, and R. Thomale, Topolectrical Circuits, Commun. Phys. **1**, 39 (2018).

[65] C. H. Lee *et al.*, Imaging nodal knots in momentum space through topolectrical circuits, Nat. Commun. **11**, 4385 (2020).

[66] P. Delplace, T. Yoshida, and Y. Hatsugai, Symmetry-Protected Multifold Exceptional Points and Their Topological Characterization, Phys. Rev. Lett. **127**, 186602 (2021)

[67] I. Mandal and E. J. Bergholtz, Symmetry and Higher-Order Exceptional Points, Phys. Rev. Lett. **127**, 186601 (2021).